Annual Journal of Hydraulic Engineering, JSCE, VOL.42, 1998, February

APPLICATION OF LINEAR AND NON-LINEAR k-ε MODELS TO FLOWS AROUND SPUR DIKES

Jing PENG [1] and Yoshihisa KAWAHARA [2]

[1] Graduate student, Dept. of Civil Engineering, University of Tokyo (Hongo 7-3-1, Bunkyo-ku, Tokyo 113, Japan)

[2] Member of JSCE, Dr. of Eng., Associate Professor, Dept. of Civil Engineering, University of Tokyo (Hongo 7-3-1, Bunkyo-ku, Tokyo 113, Japan)

This paper is concerned with three-dimensional numerical analysis of turbulent flows around submerged spur-dikes. A finite volume method is employed to discretize the governing equations. A nonlinear k-ε model proposed by Shih et al. and a linear k-ε model modified by Zhu-Shih are applied to two cases of flow with different spur dikes. The comparison with measured data shows that the nonlinear k-ε model reproduces mean velocity field better than the modified linear k-ε model in the two cases. The reason of the superiority of the non-linear model is discussed. It is shown, however, that further improvement in the numerical model is required to reproduce the complex flow phenomena accurately.

Key Words: *spur dikes, turbulent flow, linear k- ε model, non-linear k- ε model, three-dimensionality*

1. INTRODUCTION

Spur dikes have been widely used in rivers to protect riverbanks from erosion during floods and improve navigability at low water flow condition. Recently they have also been used to improve aquatic habitat by providing and maintaining stable pools and diverse flow environment. More attention has been paid to the investigation of flow structure and the associated erosion process by physical and numerical models. Two-dimensional[1] and three-dimensional numerical models[2] have been developed and applied to predict the flowfield at the presence of submerged spur dikes and transport phenomena around them. But the flow characteristics are not yet well understood and poorly predicted by the numerical models, since the flowfield shows highly three-dimensional complexity and unsteadiness, hence is difficult to predict accurately.

In this study, we compare the performance of a non-linear k-ε model devised by Shih et al.[3] and that of a linear k-ε model modified by Zhu-Shih[4] to single out a reliable turbulence model to reproduce the flow around submerged spur dikes. The linear k-ε model is found to the most reliable one among several linear k-ε models[2], even though it shows some discrepancies compared with experimental results. The present study aims to confirm the higher reliability of the non-linear k-ε model when applied to flow in open channel with spur dikes, with the hope that it may server as a flow model when we predict scouring processes and sediment transport.

2. NUMERICAL SIMULATION

(1) Governing Equations

The governing equations for three-dimensional incompressible steady turbulent flow are the continuity equation and three momentum equations that are expressed as:

$$\frac{\partial U_i}{\partial x_i} = 0 \tag{1}$$

$$U_j \frac{\partial U_i}{\partial x_j} = -\frac{1}{\rho}\frac{\partial P}{\partial x_i} - g\frac{\partial Z_b}{\partial x_i} + \frac{\partial}{\partial x_j}\left(\nu \frac{\partial U_i}{\partial x_j} - \overline{u_i u_j}\right) \tag{2}$$

where U_i is the mean velocity, P the pressure and Z_b the bed level. In the linear k-ε model, the Reynolds stresses $-\overline{u_i u_j}$ are expressed using eddy viscosity concept as:

$$-\overline{u_i u_j} = \nu_t\left(\frac{\partial U_i}{\partial x_j} + \frac{\partial U_j}{\partial x_i}\right) - \frac{2}{3}k\delta_{ij} \tag{3}$$

$$\nu_t = c_\mu \frac{k^2}{\varepsilon} \tag{4}$$

where k is the turbulent kinetic energy and ε is its dissipation rate. The values of k and ε are calculated through their transport equations that are written as:

$$U_j \frac{\partial k}{\partial x_j} = \frac{\partial}{\partial x_j}\left[\left(\nu + \frac{\nu_t}{\sigma_k}\right)\frac{\partial k}{\partial x_j}\right] + \mathrm{Pr}od - \varepsilon \quad (5)$$

$$U_j \frac{\partial \varepsilon}{\partial x_j} = \frac{\partial}{\partial x_j}\left[\left(\nu + \frac{\nu_t}{\sigma_\varepsilon}\right)\frac{\partial \varepsilon}{\partial x_j}\right] + \frac{\varepsilon}{k}\left(C_{\varepsilon 1}\,\mathrm{Pr}od - C_{\varepsilon 2}\varepsilon\right) \quad (6)$$

$$\mathrm{Pr}od = -\overline{u_i u_j}\frac{\partial U_i}{\partial x_j} \quad (7)$$

It is well recognized that the standard k-ε model widely used overpredicts the eddy viscosity in the regions of flow separation and recirculation. To minimize this weak points, a modification was proposed by Zhu-Shih[4] where the model coefficients are determined as:

$$c_{\varepsilon 1} = 1.44,\ c_{\varepsilon 2} = 1.92,\ \sigma_k = 1.0,\ \sigma_\varepsilon = 1.3,\ c_\mu = \frac{2/3}{5.5 + \eta} \quad (8)$$

where

$$\eta = \frac{Sk}{\varepsilon},\ S = \left(2S_{ij}S_{ij}\right)^{1/2},\ S_{ij} = \frac{1}{2}\left(\frac{\partial U_i}{\partial x_j} + \frac{\partial U_j}{\partial x_i}\right) \quad (9)$$

Based on a realizability analysis of turbulent normal stresses, the functional form for c_μ in Eq. (8) is derived in terms of the time scale ratio of turbulence to the mean flow. The coefficient c_μ modifies the value of eddy viscosity ν_t to work better than the standard k-ε model.

In order to predict accurately the anisotropy of turbulent stresses, which contributes significantly to the generation and transport of vortices and the secondary motion and in return affects the mean flow feature, a nonlinear stress-strain relation must be introduced. Shih et al.[3] suggested quadratic stress-strain relation, which is achieved under the constraint of rapid distortion theory for the rapid rotation and the realizability condition. A non-linear algebraic Reynolds-stress expression in this model is written as:

$$\overline{u_i u_j} = \frac{2}{3}k\delta_{ij} - C_\mu \frac{k^2}{\varepsilon}2S_{ij}^* + 2C_2\frac{k^3}{\varepsilon^2}\left(-S_{ik}^*\Omega_{kj}^* + \Omega_{ik}^*S_{kj}^*\right) \quad (10)$$

The coefficients C_μ and C_2 are determined from the following relations:

$$C_\mu = \frac{1}{6.5 + A_s^* U_s^*(k/\varepsilon)},\quad C_2 = \frac{\sqrt{1 - 9C_\mu^2(S^*(k/\varepsilon))^2}}{1 + 6S^*\Omega^*(k^2/\varepsilon^2)} \quad (11)$$

where

$$S^* = \sqrt{S_{ij}^*S_{ij}^*},\quad \Omega^* = \sqrt{\Omega_{ij}^*\Omega_{ij}^*},$$

$$U^* = \sqrt{S_{ij}^*S_{ij}^* + \Omega_{ij}^*\Omega_{ij}^*},\quad W^* = \frac{S_{ij}^*S_{jk}^*S_{ki}^*}{(S^*)^3}, \quad (12)$$

and

$$S_{ij}^* = S_{ij} - \frac{1}{3}S_{kk}\delta_{ij},\quad \Omega_{ij}^* = \Omega_{ij},$$

$$S_{ij} = \frac{1}{2}\left(\frac{\partial U_i}{\partial x_j} + \frac{\partial U_j}{\partial x_i}\right),\quad \Omega_{ij} = \frac{1}{2}\left(\frac{\partial U_i}{\partial x_j} - \frac{\partial U_j}{\partial x_i}\right), \quad (13)$$

$$A_s^* = \sqrt{6}\cos\phi_1,\quad \phi_1 = \frac{1}{3}\arccos\left(\sqrt{6}W^*\right)$$

The coefficients $C_{\varepsilon 1}$, $C_{\varepsilon 2}$, σ_k and σ_ε are specified to take the same values as the standard linear model:

$$C_{\varepsilon 1} = 1.44,\quad C_{\varepsilon 2} = 1.92,\quad \sigma_k = 1.0,\quad \sigma_\varepsilon = 1.3 \quad (14)$$

(2) Numerical method

All the equations are discretized by the finite volume method on a staggered grid system where the grids near the spur dikes are clustered. To ensure both accuracy and stability of numerical solution, the convection terms are handled by a second order and consistently formulated QUICK scheme suggested by Hayase et al[5]. Diffusion terms are discretized by the central difference scheme. The velocity-pressure coupling is solved with the SIMPLE algorithm. Convergence criteria are set such that the maximum normalized residual of all dependent variables is less than 10^{-4}.

(3) Boundary conditions and initial conditions

Boundary conditions should be given at inlet, outlet, free surface and wall boundaries. The velocity components and turbulence quantities are specified at inlet. At the downstream end, the longitudinal gradients of all the variables are assumed to be zero. Free surface is treated as a symmetry plane. Along wall boundaries including bed and side walls of channel and all faces of spur dikes, the wall function approach is used to bridge the viscous sublayer in order to alleviate fine grids requirement due to high velocity gradient near wall region. Initial conditions are prepared by solving the equations of continuity and momentum in the absence of viscosity effect to reduce the total computational time.

3. APPLICATION TO EXPERIMENT

(1) Flow around an isolated submerged spur dike

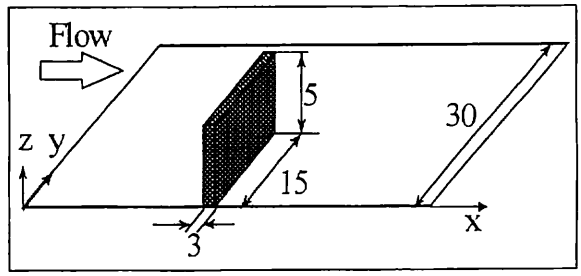

Fig.1 Flow over a spur dike (unit: cm).

flow currents in this area. Strong separated flow released from the tip face of spur dikes shift the maximum velocity towards the opposite side wall. This point requires further verification.

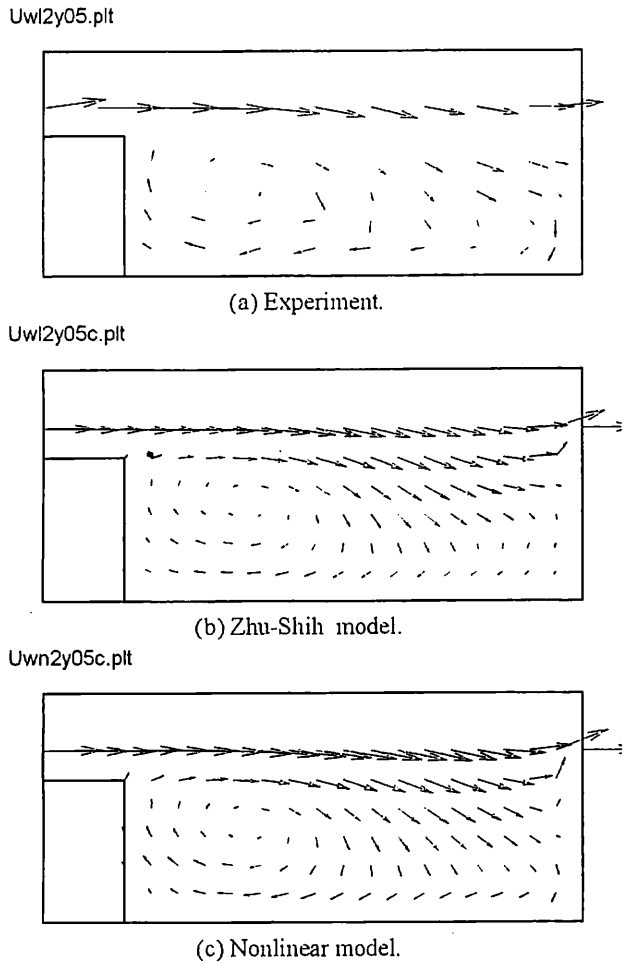

(a) Experiment.

(b) Zhu-Shih model.

(c) Nonlinear model.

Fig. 7 Comparison of U-W vectors.

Recirculation flow pattern between two spur dikes is presented by plotting the dimensionless U-W vectors in a vertical plane (V-plane as shown in Fig. 5). Fig. 7 compares the experimental result and the simulated results with the two models. The general recirculating flow pattern at the back of the spur dike is well predicted by both linear and nonlinear models. Compared with the flow around a single spur dike, it can be seen that the flow feature around spur dikes in series shows different pattern. This is due to the effects of downstream spur dike on the recirculation flow structure. It is natural and the experiment also shows that the interval of spur dikes is one of the parameters controlling the flow structure for flow over spur dike system. Physical and numerical models are both needed to well understand the complex flow characteristics.

Direct comparison of the calculated turbulent quantities, such as the turbulent kinetic energy and Reynolds stresses, is not executed in the present paper because electro-magnetic velocimetry fails to offer the reliable experimental data of turbulent quantities for this study case. We compared hereafter only the results between the two numerical models on the distributive feature of turbulence energy. Based on the comparison results of the mean streamwise velocity we can analyze the effects of turbulence energy k on the distribution of mean velocity.

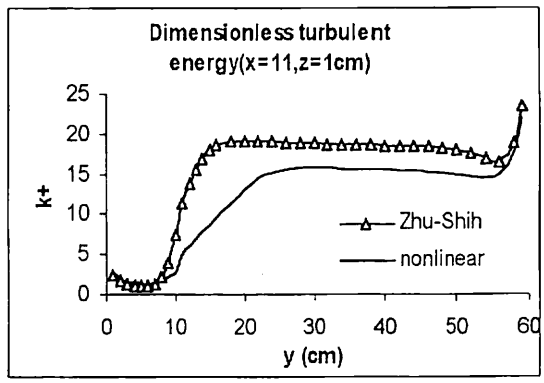

Fig. 8 Dimensionless turbulent kinetic energy.

Fig. 8 depicts the dimensionless k profiles by the two models along the same spanwise line as in Fig. 6(b). Turbulence energy k is normalized here by the upstream mean velocity U_m as $k^+=100 \cdot k/U_m^2$. The results show that Zhu-Shih model yields a high level and a sharp increase of turbulence energy k in the tip region (around y=10cm~20cm), where it overpredicted the mean velocity as mentioned above. Contrarily the nonlinear model gives a lower level of turbulence energy with a relative slight increase of k in this region.

It is likely that the overprediction of the mean streamwise velocity in the tip region of spur dikes by the Zhu-Shih model is related to the overprediction of turbulent quantities. It has been reported that a reliable turbulent model is indispensable to reproduce the flow around spur dikes accurately[7], because the turbulent motion dominates the flow behavior in the near region. Analytically the improved distribution in streamwise mean velocity by the nonlinear model is attributed to more accurate representation of Reynolds stresses.

4. CONCLUSIONS

A fully three-dimensional nonlinear k-ε model and a linear modeified k-ε model are applied to flows around a submerged single spur dike and spur dikes in series. The results are compared with the experimental data. The general recirculating flow pattern at the back of the spur dike is well predicted by both linear and nonlinear models. The comparison

Tominaga and Chiba[6] measured three velocity components over a submerged spur dike in a straight flume. The geometry of the flow domain is schematically shown in Fig. 1. The x-coordinate is aligned in the streamwise direction, y-coordinate in the spanwise direction and z-coordinate in the vertical direction. The flume has a length of 8m. An isolated spur dike is located at x=4m. Flow discharge is 3,600cm^3/s with a water depth of around 9cm.

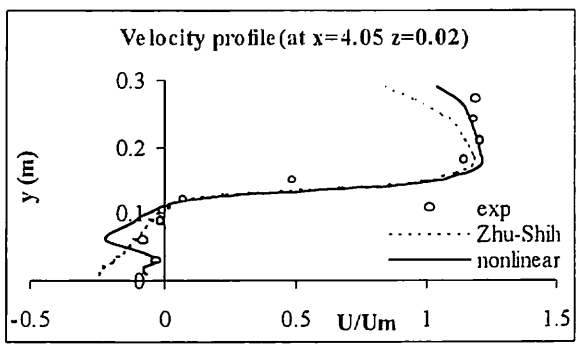

(a) At x=4.05m, z=0.02m.

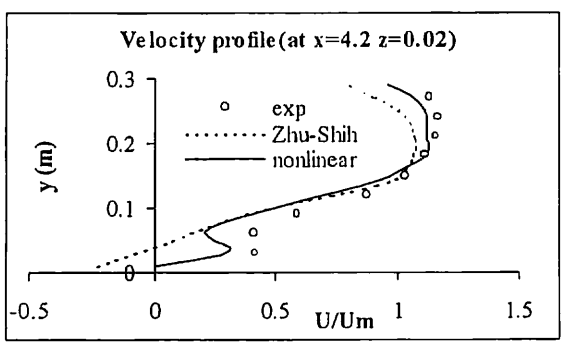

(b) At x=4.2m, z=0.02m.

Fig.2 Plan view of the streamwise mean velocity profiles.

Flow conditions in the calculation are the same with the experiment. The three-dimensional grid system has 147×47×20 nodal points. Fig. 2(a) and (b) compare the calculated streamwise mean velocity profiles among the linear Zhu-Shih k-ε model, the non-linear k-ε model and the experimental data at two different downstream locations in the horizontal plane 2cm above bed. The linear Zhu-Shih model underestimates the mean velocity in the tip region downstream of the spur dike (around y >0.15m in Fig. 2(a) and (b)). This means the underprediction of separation currents in the tip area of spur dike. Since it is the separation currents that play an important role in the local scour frequently encountered in the tip area of spur dikes, the underprediction of separation currents influences the proper estimation of local scour. The nonlinear model yields better results than the linear model for the velocity in this region. Behind the spur dike where reverse current is active the predictions show some differences with the experiment. The nonlinear model predicts stronger reverse flows than the experiment, giving a larger negative peak value around y=0.06m in Fig. 2(a).

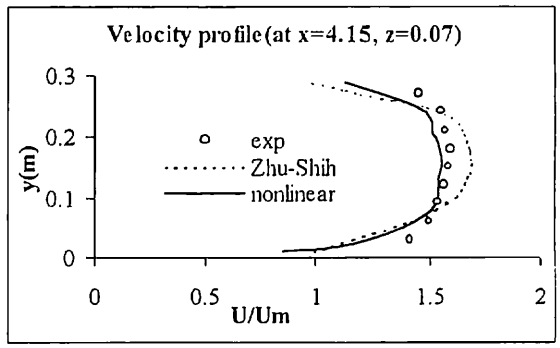

Fig. 3 Velocity profiles (at x=4.15m, z=0.07m).

Fig.3 shows the streamwise velocity profiles downstream the spur dike in the horizontal plane 7cm above bed (around 2cm below free surface) together with the experimental data. Again the nonlinear model gives more reasonable results with the experiment while the linear model overpredicts the mean velocity in the center part of the flume and underpredicts it near both side walls.

uvgeh1.plt

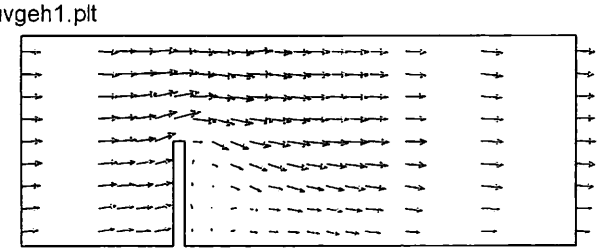

(a) Experiment.

uvg2-1h1.plt

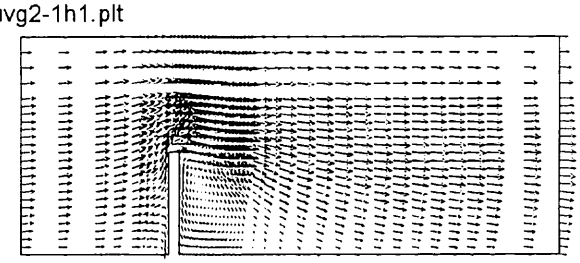

(b) Zhu-Shih model.

uvg2-2h1.plt

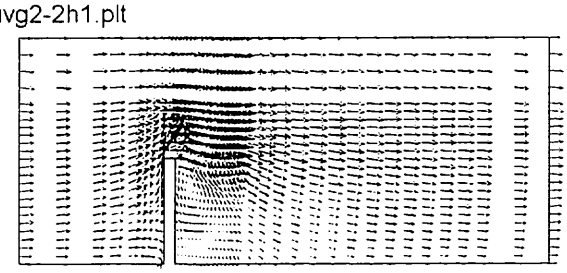

(c) Non-linear model.

Fig. 4 U-W vectors near bed wall (z=0.02m).

Fig. 4(a), (b) and (c) show the comparison of calculated and measured U-V vectors near the bed wall (2cm above the bed) in non-dimensionized form by the cross-sectional mean velocity. The experiment gives the reattachment length of about 0.7 L_g, where L_g is the length of spur dike in spanwise direction. The linear model and nonlinear model predict $1.0L_g$ and $0.8L_g$ respectively, both overpredict this length to some degree.

From the above comparison, it can be said that the nonlinear k-ε model yields more reasonable results than the linear k-ε model in this case.

(2) Flow around submerged spur dikes in series

The main function of spur dike is to provide riverbank protection. In many practices, spur dikes are arranged not in isolated way but in series to function as a spur dike system for efficient the riverbank protection. The flow structure and sediment transport phenomena become more complicated in this situation because of the interaction of each spur dike flow. It is of practical importance for a numerical model to predict the flow characteristics therefore to support the design work of spur dikes.

The nonlinear k-ε model and the linear Zhu-Shih k-ε model are applied to the flow around submerged spur dikes. The results are also compared with the experiment carried out by the authors.

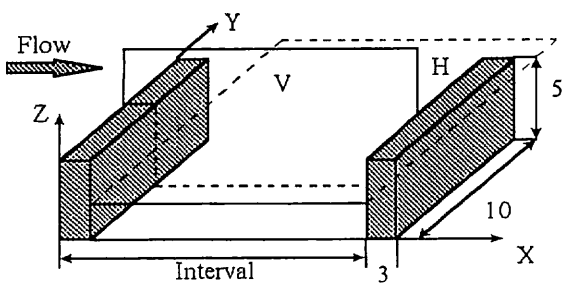

Fig. 5 Flow over spur dikes in series(unit: cm).

The experiment is conducted in a straight flume with bed slope 1/750. The flume has the length of 10m and the width of 0.6m. Many spur dikes of the same size ($3\times10\times5$ cm^3) are installed along one side bank at same interval. Measuring section is placed where the flow is fully developed to show periodic characteristics. Fig. 5 shows the measuring section between two spur dikes and the coordinate system in the numerical simulation. Measuring items include three velocity components by electro-magnetic velocimetry and water depth by an automatic stage probe. The flow discharge is 21.3 l/s with the water depth around 8.0cm in the middle part of flume. Three cases of different spur dike interval are tested in the experiment. The results in one case with spur dike interval of 20cm are presented here and compared with the numerical results.

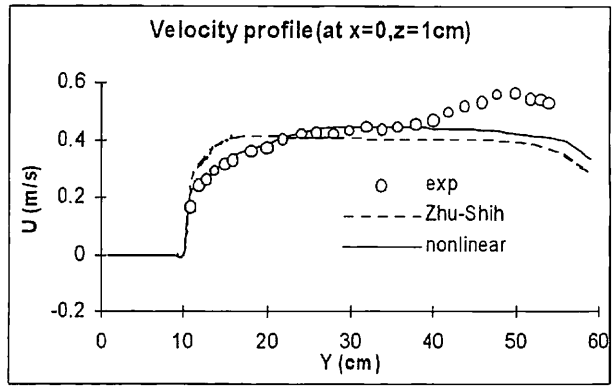

(a) At x=0cm, z=1cm

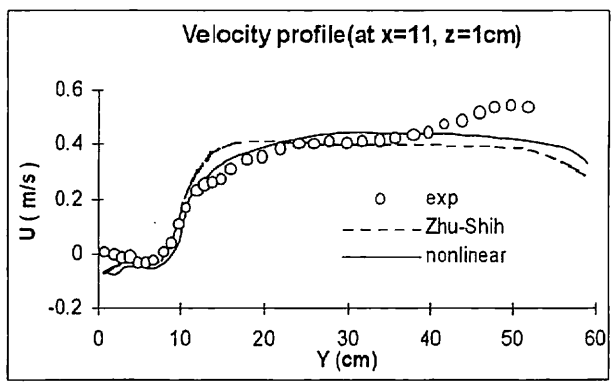

(b) At x=11cm, z=1cm

Fig. 6 Streamwise mean velocity profiles.

Fig. 6 (a) and (b) give the comparison of the streamwise mean velocity profiles by the two models with the experiment. The section x=0.0cm locates at the upstream face of first spur dike and the section x=11.0cm stands in the recirculation region between two spur dikes. Both are the results in the horizontal plane at z=1cm above bed.

The result shows that the linear k-ε model overpredicts the velocity in the tip region of spur dikes (around y=10~20cm). The non-linear model significantly improves the prediction in this region. The velocity agrees very well with the experiment. The two models, however, underestimate the velocity and miss the peak value of mean velocity near the opposite side wall (around y=40~60cm), which is apparent in the measured data. The reason of why there exists large difference in the mean streamwise velocity in this region between the calculation and experiment remains unclear. The appearance of the peak value of the mean velocity near the opposite side wall in the measured data also deserves explanation. It may partly be the result of the secondary

results show that the nonlinear k-ε model predicts the mean velocity field around spur dikes reasonably better than the linear model in both cases. The reason is ascribed to more reasonable presentation of Reynolds stresses in the nonlinear model. The effect of spur dikes on the opposite side wall is strong in the experiment, resulting in the deformation of velocity profile with a peak value near the opposite side wall. But both linear and nonlinear model do not capture this feature. Further improvement in the numerical model to reproduce the complex flow feature accurately is required.

ACKNOWLEDGMENT: The authors gratefully acknowledge that Dr. A. Tominaga generously offered the present study with his experimental data and that this study is partially supported by the foundation for River Environment Management.

REFERENCES

1) S. Fukuoka, T. Nishimura and A. Kawaguchi, Numerical analysis of the flow around submerged groins, *Proc. Symp. on River Hydraulics and Environments*, 211-216,1995.

2) Y. Kawahara and J. Peng, Three-dimensional numerical simulation of flood flows around groins, *Proc. 2nd Asian Computational Fluid Dynamics Conference*, 2, 539-544, 1996.

3) T. H. Shih, J. Zhu and J. L. Lumley, A new Reynolds stress algebraic equation model, *Comput. Methods Appl. Mech. Eng.*, 125, 287-302, 1995.

4) J. Zhu and T. H. Shih, Calculations of turbulent separated flows with two-equation turbulence models, *Computational Fluid Dynamics JOURNAL*, 3, 343-354, 1994.

5) T. Hayase, J. A. C. Humphrey and R. Greif, A consistently formulated QUICK scheme for fast and stable convergence using finite-volume iterative calculation procedures, *Journal of Computational Physics*, 98, 108-118, 1992.

6) A. Tominaga and S. Chiba, Flow structure around a submerged spur dike, *Proc. of Annual Meeting of Japan Society of Fluid Mechanics*, 317-318, 1996.

7) J. Peng, Y. Kawahara and N. Tamai , Numerical analysis of three-dimensional turbulent flows around submerged groins. *Proc. 27th IAHR Congress*, A, 244-249, 1997.

(Received September 30,1997)